Food Chemistry 230 (2017) 306–315

Contents lists available at ScienceDirect

Food Chemistry

journal homepage: www.elsevier.com/locate/foodchem

Protective property of mulberry digest against oxidative stress – A potential approach to ameliorate dietary acrylamide-induced cytotoxicity

Linxia Zhang [1], Yang Xu [1], Yuting Li, Tao Bao, Vemana Gowd, Wei Chen *

Department of Food Science and Nutrition, Zhejiang Key Laboratory for Agro-Food Processing, Key Laboratory of Agro-Products Postharvest Handling, Ministry of Agriculture, National & Local Joint Engineering Laboratory of Intelligent Food Technology and Equipment, Zhejiang University, Hangzhou 310058, China

ARTICLE INFO

Article history:
Received 8 October 2016
Received in revised form 8 March 2017
Accepted 8 March 2017
Available online 9 March 2017

Keywords:
Mulberry digest
Acrylamide
Cytotoxicity
Oxidative stress
Phenolic compounds

ABSTRACT

The aim of this study was investigating the protective effect of mulberry digest (MBD) on acrylamide-induced oxidative stress. Composition analysis of MBD revealed that it contained six major phenolic compounds (quercetin-3-*O*-rutinoside, quercetin hexoside, quercetin rhamnosylhexoside hexoside, kaempferol rhamnosylhexoside, cyanidin-3-*O*-glucoside and cyanidin-3-*O*-rutinoside). After *in vitro* digestion, the contents of two anthocyanins were both decreased significantly, while the contents of four flavonoid glycosides were all increased. In addition, MBD was found to successfully suppress acrylamide-induced ROS overproduction, restore the mitochondrial membrane potential, and inhibit the mitochondrial membrane lipid peroxidation and glutathione depletion. More interestingly, the protective effect of MBD against acrylamide-induced oxidative damage was enhanced compared with mulberry fruits without digestion (MBE). Further study revealed that MBD enhanced the cell resistance capacity to acrylamide-induced oxidative stress, rather than its direct reaction with acrylamide. Overall, our results indicate that MBD provides a potent protection against acrylamide-induced oxidative stress.

1. Introduction

Acrylamide (ACR) is colorless and odorless crystalline powder and it was classified as Group 2A carcinogen by the International Agency for Research on Cancer (IARC) in 1994. In 2002, ACR was widely detected in carbohydrate-rich foods like biscuits, fried potatoes and coffee. Maillard reaction between asparagine and reducing sugars during bakery food processing leads to formation of ACR. Statistically it was proved that human exposure to bakery products increased globally and due to presence of toxic substances such as ACR, in a long run exposure to bakery food products could have a negative impact on human health such as genotoxicity, cytotoxicity and neurotoxicity (Prasad & Muralidhara, 2012). Therefore, exposure of humans to ACR through their diet should not be neglected.

Recent studies on ACR revealed that the mitochondrial dysfunction and oxidative stress are the major mechanisms involved in its cytotoxicity and genotoxicity (Halliwell, 2006). Overproduction of reactive oxygen species (ROS) or an abrogation of antioxidant defense system could disturb cellular redox balance, resulting in cell injury or apoptosis. Studies from Chen et al. demonstrated that incubation of Caco-2 cells with acrylamide for 24 h accelerated the level of ROS and decreased the cell viability (Chen, Shen, Su, & Zheng, 2014; Chen, Su, Xu, Bao & Zheng, 2016). Therefore, the viable strategies to ameliorate ACR-induced toxicity are urgently needed. Among these strategies, natural antioxidants derived from vegetables and fruits that are capable of scavenging ROS and maintaining cellular redox balance have received more attention (Chen et al., 2011; Rodriguez-Ramiro, Ramos, Bravo, Goya, & Angeles Martin, 2011). Distribution of bioactive compounds in berry family fruits were extensively studied so far. For instance, raspberry, bayberry and mulberry fruits are found to be rich in phytochemicals such as anthocyanins, flavonoids, and phenolic acids, with extended biological and pharmacological importance (Chen, Su, Huang, Feng, & Nie, 2012; Natic et al., 2015; Wu, Tang, et al.,

Abbreviations: MBD, mulberry digest; MBE, mulberry extract; ACR, acrylamide; C3G, cyanidin-3-*O*-glucoside; C3R, cyanidin-3-*O*-rutinoside; ROS, reactive oxygen species; MMP, mitochondrial membrane potential; GSH, glutathione; CAT, catalase; SOD, superoxide dismutase.

* Corresponding author.
E-mail address: zjuchenwei@zju.edu.cn (W. Chen).

[1] The two authors contributed equally to this work.

http://dx.doi.org/10.1016/j.foodchem.2017.03.045
0308-8146/

2013). ROS inhibition studies revealed that myricitrin which prepared from bayberry was effectively inhibited the ROS generation and reduced its associated oxidative damage (Chen, Feng, et al., 2013; Chen, Zhuang, Li, Shen, & Zheng, 2013). Anthocyanins were the major components involved in the amelioration of oxidative stress *via* diminution of ROS production (Wu, Qi, et al., 2013). Moreover mulberry fruits extracts were demonstrated with potent hypolipidemic (Liu et al., 2009), hypoglycemic (Yan, Zhang, Zhang, & Zheng, 2016) and antioxidant (Yang, Yang, & Zheng, 2010) activities. However, mulberry fruits are supposed to go through the extreme gastrointestinal digestive process before it admits actual biological activity. During the process there are chances of trapping of bioactive compounds in mulberry matrix, further leading to formation of inactive compounds and other unusual bioactive compounds. Hence, consideration of simulated gastrointestinal digestion prior to assessment of biological activity of mulberry fruits is recommended. Therefore, in this study, we aimed to produce mulberry digest by *in vitro* simulated gastrointestinal digestion, and further investigate the protective effect of mulberry digest against ACR-induced oxidative damage in HepG2 cells.

2. Materials and methods

2.1. Materials and reagents

Mulberry fruits (*Morus alba L.*) were purchased from a local market in Hangzhou, China. Fresh fruits were washed with sterile distilled water and then dried at room temperature to remove the surface water. After that, fresh fruits of same size and integrity were screened and then stored at −80 °C prior to use.

Hoechst 33342, 3-(4,5-dimethyl-2-thiazolyl)-2,5-diphenyl-2-H-tetrazolium bromide (MTT), Rhodamine 123 (RH123), 2′,7′-dichlor ofluorescin diacetate (DCFH-DA), Nonyl Acridine Orange (NAO), Naphthalene-2, 3-dicarboxal-dehyde (NDA), cyanidin-*3-O*-glucoside, cyanidin-*3-O*-ruitnoside, quercetin-*3-O*-rutinoside (rutin), acrylamide, Folin & Ciocalteu's phenol reagent, pepsin, pancreatin and bile salts were purchased from Sigma-Aldrich (St. Louis, MO, USA). BCA protein assay kit, cell lysis buffer, total superoxide dismutase assay kit and catalase assay kit were purchased from Beyotime Institute of Biotechnology., Ltd (Shanghai, China). All other reagents were of analytical grade.

2.2. In vitro simulated gastrointestinal digestion

The simulated gastrointestinal digestion was performed as detailed in earlier reports with slight modification (Kremer Faller, Fialho, & Liu, 2012). In brief, 10 g of mulberry fruits were homogenized with 5 mL of distilled water and then diluted to 20 mL for gastric digestion. Prior to gastric digestion, the solution was acidified to pH 2 using 5 M HCl, and porcine pepsin (6000 units) was added subsequently. After that, the mixture was kept for incubation in a shaking water bath (100 rpm) at 37 °C for about 90 min. After incubation the pH of the mixture was adjusted to pH 6.5 by adding 1 M sodium bicarbonate and further 5 mL of pancreatin was added (consisting of 4 mg/mL trypsin and 25 mg/mL porcine bile salts), followed by adjusting pH to 7.4 using 1 M sodium hydroxide before subjecting to intestinal digestion. Thereafter, the mixture was incubated in a shaking water bath (100 rpm) at 37 °C for 2 h. At the end of intestinal digestion, the mixture was diluted to a final volume of 30 mL with distilled water and then centrifuged for 10 min at 5000 rpm and supernatant was collected. The supernatant was referred to as MBD and was stored at −80 °C until use. As for preparation of mulberry fruits without digestion, 10 g of mulberry fruits were homogenized with 5 mL of distilled water and then diluted to a final volume of 30 mL with distilled water, followed by centrifuging for 10 min at 5000 rpm. The supernatant was collected and stored at −80 °C prior to use.

2.3. Assessment of anthocyanins in mulberry digest (MBD) by HPLC

Determination of anthocyanins in mulberry digest (MBD) was performed by HPLC-DAD (Dionex ultimate 3000, ThermoFisher Scientific, USA) and relevant standard (cyanidin-*3-O*-glucoside and cyanidin-*3-O*-rutinoside) were used. Briefly mobile phase A consists of formic acid and water (8.5:91.5, v/v) and mobile phase B consists of formic acid, methanol, acetonitrile and water (8.5:22.5:22.5:41.5, v/v/v/v). The elution was carried out at 30 °C on a Promosil C18 column (4.6 × 250 mm, 5 μm, Bonna-Agela Technologies, Tianjin, China), with flow rate of 1 mL/min, in the following linear gradient: from 93% to 75 % A for 35 min, from 75% to 35% A for 10 min, from 35% to 0% A for 1 min, 100% B for 4 min. The detection wavelength was set to 520 nm and the injection volume was 10 μL.

2.4. Identification of phenolic compounds by UPLC-Triple-TOF-MS

Identification of phenolic compounds in mulberry digest (MBD) was performed using an UPLC system (Acquity™, Waters, USA) connected to Triple-TOF Mass Spectrometry System (AB SCIEX, Triple-TOF 5600plus Framingham, USA). The elution was carried out at 30 °C on a Promosil C18 column (4.6 × 250 mm, 5 μm). The mobile phase consists of acetonitrile (A) and 0.1% aqueous formic acid solution (B), with flow rate of 0.8 mL/min, in the following linear gradient: 5% A for 5 min, from 5% to 16% A for 20 min, from 16% to 30% A for 8 min, from 30% to 90% A for 2 min, 90% A for 5 min, from 90% to 5% A for 5 min and then isocratic elution for 5 min. The detection wavelength was set to 360 nm, with injection volume 10 μL. MS spectra was obtained by full range acquisition covering the *m*/*z* range 50–2000 in negative ion mode, with the voltage and source temperature reached to 4.5 kV and 550 °C, respectively.

2.5. Quantitative analysis

Quantitative analysis of major components was performed using commercial available analytical standards. For anthocyanin quantification, cyanidin-*3-O*-glucoside and cyanidin-*3-O*-rutinoside were used as standards. For quercetin or quercetin derivatives quantification, quercetin-*3-O*-rutinoside (rutin) was used as a standard. The contents of other quercetin derivatives were expressed as quercetin-*3-O*-rutinoside equivalent.

2.6. Cell culture

Human HepG2 cells were obtained from Cell Bank of Type Culture Collection of Chinese Academy of Sciences. Cells were cultured in RPMI 1640 medium (Gibco) consisting of 100 units/mL streptomycin, 100 units/mL penicillin and 10% of the new calf serum and incubated in a humidified atmosphere with 5% CO_2 at 37 °C.

2.7. Cell viability assay

Cell viability was evaluated by the MTT method as detailed in earlier reports (Chen, Zhao, & Li, 2011). Briefly, HepG2 cells were seeded into 96-well cell culture plates at a density of 4×10^3 cells/well and then incubated for 24 h. After incubation HepG2 cells were pretreated with MBD solution (0.25 mg/mL, 0.5 mg/mL and 1 mg/mL) for 24 h and then treated with ACR (5 mM) for another 24 h. Subsequently, MTT (0.5 mg/mL) was added to cell culture plate and incubated for 4 h. Then the generated formazan precipitate was dissolved in 150 μL of DMSO

and absorbance was measured at 490 nm using a Tecan infinite M200 microplate reader.

2.8. Cell nucleus staining

Hoechst 33258, a fluorescence dye which binds to adenine-thymine rich sites of DNA, is frequently used to study the cell nucleus morphology (Kang et al., 2014). Briefly, after treatment, cells from each group were collected and stained with 10 μM Hoechst 33258 at 37 °C for 30 min. After staining, cells were washed with PBS and observed under fluorescence microscope.

2.9. Measurement of intracellular reactive oxygen species (ROS)

Oxidation of a non-fluorescent reagent 2,7-dichlorodihydrofluorescein diacetate (DCFH-DA) leads to formation of fluorescent compound (2,7-dichlorofluorescein, DCF). This reaction was widely used to study the level of intracellular reactive oxygen species (ROS) (Chen et al., 2008). Briefly, HepG2 cells were seeded into 12-well cell culture plates at a density of 5×10^4 cells/well and incubated for 24 h. After incubation, cells were pretreated with MBD (0.5 mg/mL and 1 mg/mL) for 24 h and subsequently treated with 5 mM ACR for another 24 h. After treatment, cells were collected and incubated with 10 μM DCFH-DA at 37 °C for 30 min, then washed with PBS and subjected to evaluation by fluorescence microscope. The results were expressed as mean DCF fluorescence intensity, which was calculated on the basis of six different microscopic fields by ImageProPlus 6.0 (Media Cybernetics, Inc.) image analysis software.

2.10. Detection of mitochondrial membrane potential (MMP)

Mitochondrial membrane potential (MMP) was measured based on the retention of rhodamine 123 (RH123) (Chen, Feng, Nie, & Zheng, 2012; Chen et al., 2008). In brief, after incubation with MBD and ACR, cells were further incubated with RH123 (10 μg/mL) at 37 °C for 30 min, and subjected to multiple washings with PBS. Then the fluorescence was observed under fluorescence microscope. The results were displayed as mean RH123 fluorescence intensity, which was calculated on the basis of six different microscopic fields by ImageProPlus 6.0 software.

2.11. Detection of mitochondrial membrane lipid peroxidation

Mitochondrial membrane lipid peroxidation was detected as previously reported (Trachootham et al., 2006). Briefly, after incubation with MBD and ACR, cells were then incubated with NAO (10 μM) at 37 °C for 30 min, followed by washing with PBS. Fluorescence was observed under fluorescence microscope. The results were expressed as mean NAO fluorescence intensity, which was calculated on the basis of six different microscopic fields by ImageProPlus 6.0 software.

2.12. Estimation of reduced glutathione (GSH)

Followed by previously described method, NDA fluorescent probe was used for estimating the level of reduced GSH (Orwar, Fishman, Ziv, Scheller, & Zare, 1995). Briefly, after incubation with MBD and ACR, cells were further incubated with NDA (50 μM) at 37 °C for 30 min, then followed by multiple washings with PBS. Fluorescence was observed under fluorescence microscope. The results were expressed as mean NDA fluorescence intensity, which was calculated on the basis of six different microscopic fields by ImageProPlus 6.0 software.

2.13. Determination of intracellular catalase (CAT) activity and superoxide dismutase (SOD)

CAT activity was determined using a catalase assay kit and a bovine serum albumin protein assay kit. Briefly, according to the manufacturers' protocol, the collected cells were disrupted, centrifuged and supernatant was collected for further analysis. The protein content of supernatant was first determined prior to assessment of total CAT activity. After protein estimation, 3.5 μL of supernatant was diluted with 36.5 μL of catalase assay buffer in a 1.5 mL centrifuge tube, and then incubated with 10 μL of hydrogen peroxide solution (250 mM) for 3 min at 25 °C. Subsequently, the enzyme reaction was terminated using vortex (450 μL). Finally, 10 μL of above reaction solution was mixed with 200 μL of chromogenic working solution and then incubated for 15 min at 25 °C. The absorbance of the final reaction solution was measured at 520 nm. One enzyme activity unit of CAT was defined as the enzyme amount catalyzing 1 μmol hydrogen peroxide in one minute. The results were expressed as the fold of CAT activity of control group.

Total SOD activity was determined using a total superoxide dismutase assay kit (WST-8) and bovine serum albumin protein assay kit. Briefly, according to the manufacturers' protocol. The collected cells were disrupted, and centrifuged. Supernatant was collected and protein was estimated prior to measurement of total SOD activity. After that, 20 μL of supernatant was mixed with 160 μL of WST-8 (Enzyme working solution, provided by assay kit), followed by adding 20 μL of reaction working solution (provided by assay kit), and then incubated for 30 min at 37 °C. At the end of reaction, the absorbance was measured at 450 nm. One enzyme activity unit of SOD was defined as the enzyme amount generating 50% inhibition in the xanthine oxidase reaction system. The results were expressed as the fold of SOD activity of control group.

2.14. Determination of acrylamide content by HPLC

HPLC was performed to analyze the ACR content (Dionex Ultimate 3000 HPLC, ThermoFisher Scientific, USA, system equipped with Promosil C18 column (4.6 × 250 mm, 5 μm)). The content of ACR was determined based on the method described by Wang, with slight modification (Wang, Lee, Shuang, & Choi, 2008). In brief, the mobile phase consists of acetonitrile (A) and water (B), and the elution was carried out by the following isocratic elution program: 5% A for 15 min. The flow rate was set at 0.8 mL/min and the inject volume was 10 μL. The absorbance of ACR was detected at 260 nm.

2.15. Statistical analysis

All data are expressed as mean ± standard deviation (SD) from at least three independent experiments and analyzed by one-way ANOVA using SPSS (version19.0). $p < 0.05$ was considered statistically significant.

3. Results and discussion

3.1. Identification of phenolic compounds in mulberry digest (MBD)

Previous studies demonstrated that mulberry fruits have wide range of biological activities. However, phenolic composition and biological activities of mulberry digest (MBD) are not well established so far. In order to identify phenolic compounds in MBD, UPLC system coupled with a high resolution mass spectrometer was used. The results were summarized in Table 1 and presented in Supplementary Fig. 1. Four major absorption peaks at 360 nm

Table 1
Qualitative and quantitative analysis of phenolic compounds of mulberry fruit before and after digestion by UPLC-TOF-MS.

Peak	Rt (min)	MS	MS^2 fragment (%)	Tentative identification	Contents after digestion (mg/kg FW)	Contents before digestion (mg/kg FW)
Flavonoids						
1	21.91	711.1986	711.2062 (100%), 609.1504 (80%), 462.0821 (40%), 301.0354 (45%), 299.0199 (80%), 271.0244 (15%)	Quercetin rhamnosylhexoside hexoside	11.05 ± 1.10	7.93 ± 2.13
2	31.25	609.1458	609.1493 (25%), 301.0360 (40%), 300.0278 (100%), 271.0253 (25%), 255.0303 (15%), 151.0040 (5%)	Quercetin-*3*-*O*-rutinoside	53.95 ± 2.21	25.01 ± 2.56
3	32.14	463.0875	463.0902 (10%), 301.0359 (35%), 300.0276 (100%), 271.0242 (75%), 255.0291 (35%), 243.0292 (15%), 151.0029 (10%)	Quercetin hexoside	5.76 ± 0.45	4.80 ± 1.27
4	32.69	593.1506	593.1560 (30%), 285.0410 (100%), 284.0328 (55%), 255.0296 (20%), 227.0344 (10%)	Kaempferol rhamnosylhexoside	4.93 ± 0.58	2.92 ± 0.29
Anthocyanins						
5	27.94	447.0925	447.0928 (5%), 285.0393 (40%), 284.0333 (100%), 255.0290 (25%)	Cyanidin-*3*-*O*-glucoside	497.28 ± 6.81	2453.76 ± 23.96
6	32.38	593.1502	593.1651 (20%), 285.0409 (70%), 284.0329 (100%), 255.0290 (10%)	Cyanidin-*3*-*O*-rutinoside	287.20 ± 9.58	1001.51 ± 17.85

The results were expressed as mg per kg fresh weight (FW). The content of flavonoids were expressed as mg of quercetin-3-O-rutinoside equivalents per kg fresh weight (FW).

were identified (peaks 1, 2, 3 and 4) (Supplementary Fig. 1A). According to the MS information and the retention time of available standards (quercetin-*3*-*O*-rutinoside), the second peak was identified as quercetin-*3*-*O*-rutinoside (rutin). Briefly, peak 2 showed a $[M-H]^-$ ion at *m*/*z* 609.1458 with a MS/MS fragment ion at *m*/*z* 301.0360. The loss unit of 308 (609.1458–301.0360) was considered as rutinoside and the typical *m*/*z* 301.0360 was considered to quercetin (De Rosso, Panighel, Vedova, Gardiman, & Flamini, 2015; Natic et al., 2015). Besides, the retention time of quercetin-*3*-*O*-rutinoside standard was in accordance with peak 2. Similarly, the other three major peaks were tentatively identified as quercetin rhamnosylhexoside hexoside (peak 1) (Wojdylo, Nowicka, Laskowski, & Oszmianski, 2014), quercetin hexoside (peak 3) (De Rosso et al., 2015; Natic et al., 2015), and kaempferol rhamnosylhexoside (peak 4) based on their MS information and the published literatures. The typical MS/MS fragment ions at *m*/*z* 301.0359 (peak 1 and peak 3) and *m*/*z* 285.0410 (peak 4) correspond to quercetin and kaempferol, respectively. Generation of these MS/MS base peaks (*m*/*z* 301.0359 and *m*/*z* 285.0410) were resulting from the loss of hexose or rhamnosylhexose. These flavonoid glycoside contents were quantified based on standard curves of quercetin-*3*-*O*-rutinoside (rutin). As shown in Table 1, quercetin-*3*-*O*-rutinoside was found to be most abundant flavonoid glycoside in MBD, with the content of 53.95 ± 2.21 mg/kg FW. The contents of other three compounds were 11.05 ± 1.10 mg/kg FW (quercetin rhamnosylhexoside hexoside), 5.76 ± 0.45 mg/kg FW (quercetin hexoside) and 4.93 ± 0.58 mg/kg FW (kaempferol rhamnosylhexoside), respectively. In addition, two major anthocyanins were found in MBD, which were identified as cyanidin-*3*-*O*-glucoside (C3G, peak 5) and cyanidin-*3*-*O*-rutinoside (C3R, peak 6), respectively (Supplementary Fig. 1B). C3G and C3R occupied a larger proportion of the total anthocyanin of MBD, with the content of 497.28 ± 6.81 mg/kg FW (C3G) and 287.20 ± 9.58 mg/kg FW (C3R). Interestingly, we have found that, after digestion, the contents of four flavonoid glycosides (quercetin rhamnosylhexoside hexoside, quercetin-*3*-*O*-rutinoside, quercetin hexoside and kaempferol rhamnosylhexoside) were all increased, while the contents of two anthocyanins (cyanidin-*3*-*O*-glucoside and cyanidin-*3*-*O*-rutinoside) were both decreased significantly (in Table 1). It is well known that anthocyanins are not stable when exposed to alkaline environment, as a result, most of anthocyanins were degradation after *in vitro* digestion (McDougall, Fyffe, Dobson, & Stewart, 2007). The increase in the contents of four flavonoid glycosides after *in vitro* digestion could be the result of the partial digestion of the dietary fiber (Ortega, Reguant, Romero, Macia, & Motilva, 2009). Previous studies have reported the bonding of phenolic compound to fiber in wine (Saura-Calixto & Diaz-Rubio, 2007). Therefore, compared with the flavonoid glycoside content extracted under softer condition, extreme acid base condition and enzymatic treatment could lead to sufficient cellular disruption and release a part of these flavonoid glycosides associated with fiber in mulberry fruits.

3.2. Effect of MBD on ACR-induced cytotoxicity and genotoxicity in HepG2 cells

In order to evaluate the effect of MBD on ACR-induced toxicity, HepG2 cells were used. Firstly, we investigated the cytotoxicity in the presence of MBD alone at different concentrations of 0.25 mg/mL, 0.5 mg/mL and 1 mg/mL. As shown in Fig. 1A, there was no cytotoxic effect observed in HepG2 cells among these concentrations, indicating that MBD was suitable for further investigation under these concentrations. In addition, as cell strains differ in their susceptibility to ACR-induced cytotoxicity (Mehri, Abnous, Mousavi, Shariaty, & Hosseinzadeh, 2012; Zhang et al., 2012), a suitable concentration of ACR (5 mM) resulted in approximately 50 % cell viability was screened by MTT assay for the following investigation (Fig. 1B). When HepG2 cells were pretreated with MBD (0.5 mg/mL, 1 mg/mL) for 24 h, the cytotoxic effect was significantly attenuated in a dose-dependent manner compared with solely ACR-treated group, while 0.25 mg/mL MBD was not effective in ameliorating ACR-induced cytotoxicity (Fig. 1C). Their cell viabilities were 55.29 ± 1.32% (ACR-treated group), 58.42% ± 2.81% (0.25 mg/mL of MBD-treated group), 63.89% ± 2.10% (0.5 mg/mL of MBD-treated group) and 78.52% ± 5.72% (1 mg/mL of MBD-treated group). These results revealed that MBD was able to resist ACR-induced cytotoxicity at a suitable concentration (0.5 mg/mL, 1 mg/mL). Previous studies have reported that exposure to ACR could cause genotoxicity in HepG2 cells (Shan et al., 2014), we then evaluated the protective effect of MBD against ACR-induced genotoxicity using Hoechst 33258, a fluorescent dye that can sensitively bind the adenine-thymine rich sites of DNA. It can be seen from Fig. 1D that, after treatment with ACR, some bright blue dots were readily observed compared with control group, indicating that cell nucleus condensed and chromatin agglutinated (Cariddi et al., 2015). By contrast, pretreatment with MBD, especially 1 mg/mL MBD, remarkably reduced the number of bright blue dots and the fluorescence was evenly distributed. This phenomenon suggested that MBD may afford positive effect against ACR-induced DNA damage.

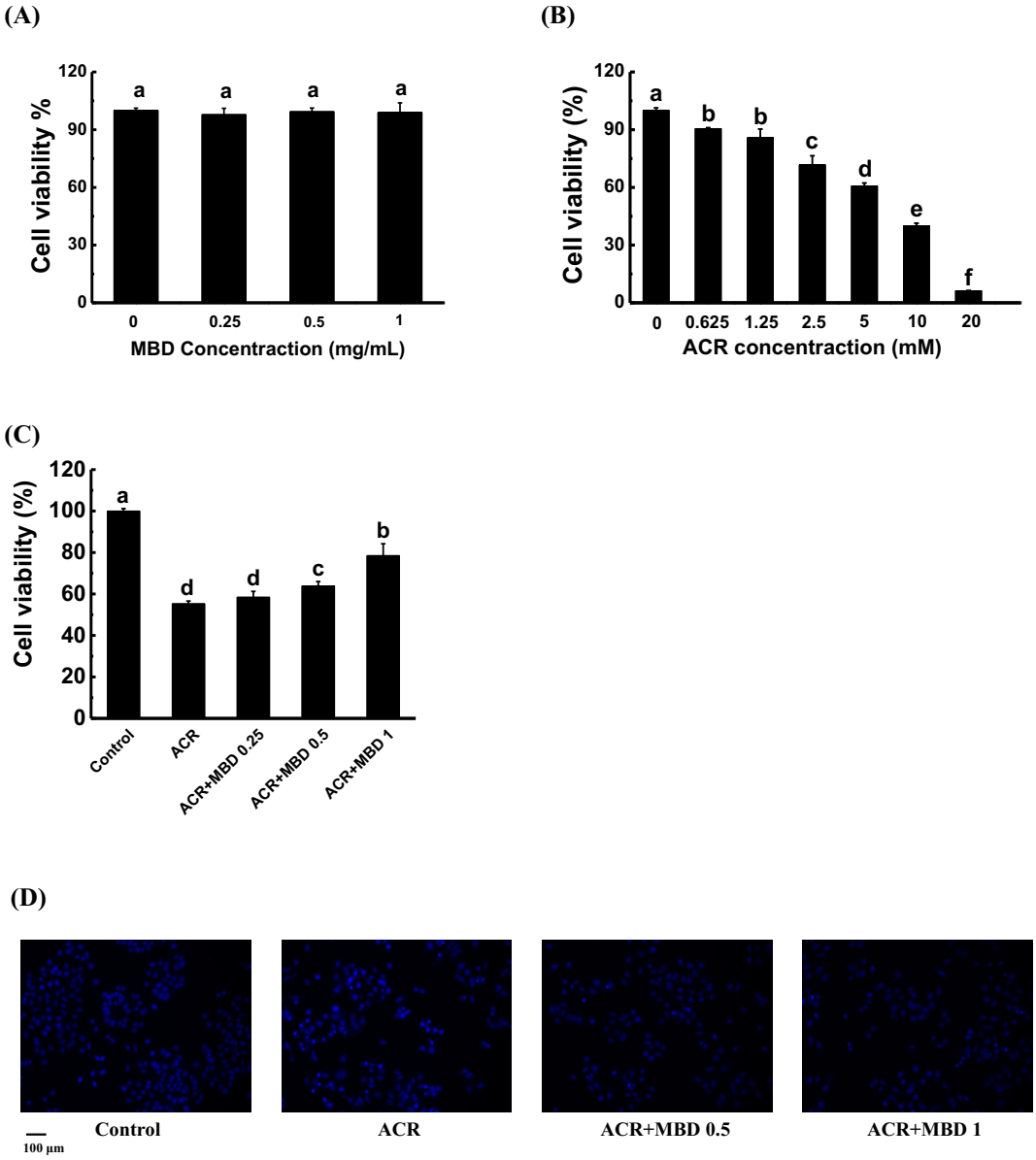

Fig. 1. Effect of MBD on ACR-induced cytotoxicity and genotoxicity. (A) The quantitative data of cell viability, HepG2 cells were treated with different concentrations of MBD (0 mg/mL, 0.25 mg/mL, 0.5 mg/mL and 1 mg/mL) for 24 h respectively, and the cell viability was determined using MTT assay. (B) The quantitative data of cell viability, HepG2 cells were treated with different concentrations of ACR ranging from 0 to 20 mM for 24 h, respectively. (C) The quantitative data of cell viability, HepG2 cells were pretreated with different concentrations of MBD for 24 h, and then incubated with ACR for another 24 h. (D) Nuclear staining of HepG2 cells with Hoechst 33342. Results were expressed as mean value ± standard deviations and different letters represent significant difference ($p < 0.05$). MBD, mulberry digest; ACR, acrylamide.

3.3. Effect of MDB on ACR-induced reactive oxygen species (ROS) generation

It is well known that overproduction of ROS leads to disturbance in cellular redox, and experimentally it was proved that supplementation of antioxidant rich sources significantly regulates the cellular redox by attenuating ROS (Rodriguez-Ramiro, et al., 2011). Therefore, we tested the effect of MBD on ACR-induced ROS generation. We measured the level of intracellular ROS in the presence or absence of MBD using DCFH-DA fluorescence staining assay. Increased fluorescence was observed (209.14% ± 11.58%) in cells which were treated with ACR for 24 h compared with non ACR-treated cells (Fig. 2A and B), indicating that ACR markedly promoted ROS generation. This was in accordance with the recent studies that exposure to ACR elevated the ROS level in PC12 cells and Caco-2 cells (Chen, Feng, et al., 2013; Mehri et al., 2012). Interestingly, pretreatment with 0.5 mg/mL, 1 mg/mL of MBD remarkably decreased the level of ROS in a dose-dependent manner, with the fluorescence intensity declined to 140.33% ± 9.59% and 108.24 ± 4.21%, respectively. More importantly, there was no significant difference between MBD-treated group (1 mg/mL) and control group (Fig. 2B), which demonstrated that MBD (1 mg/mL) could efficiently scavenge excessive ROS. In addition, we also compared the effect of mulberry fruits before (MBE, 1 mg/mL) and after digestion (MBD, 1 mg/mL) on ACR-induced ROS generation. As shown in Fig. 2C and Supplementary Fig. 8 A-8B, both MBE-treatment and MBD-treatment significantly decreased the level of ROS, with the fluorescence intensity declined to 123.13% ± 9.39% and 95.69% ± 7.89%, respectively, and MBD exhibited a better performance in scavenging intracellular ROS than MBE. According to the phenolic composition of MBD and MBE, we found that MBD and MBE are combination of various phenolic

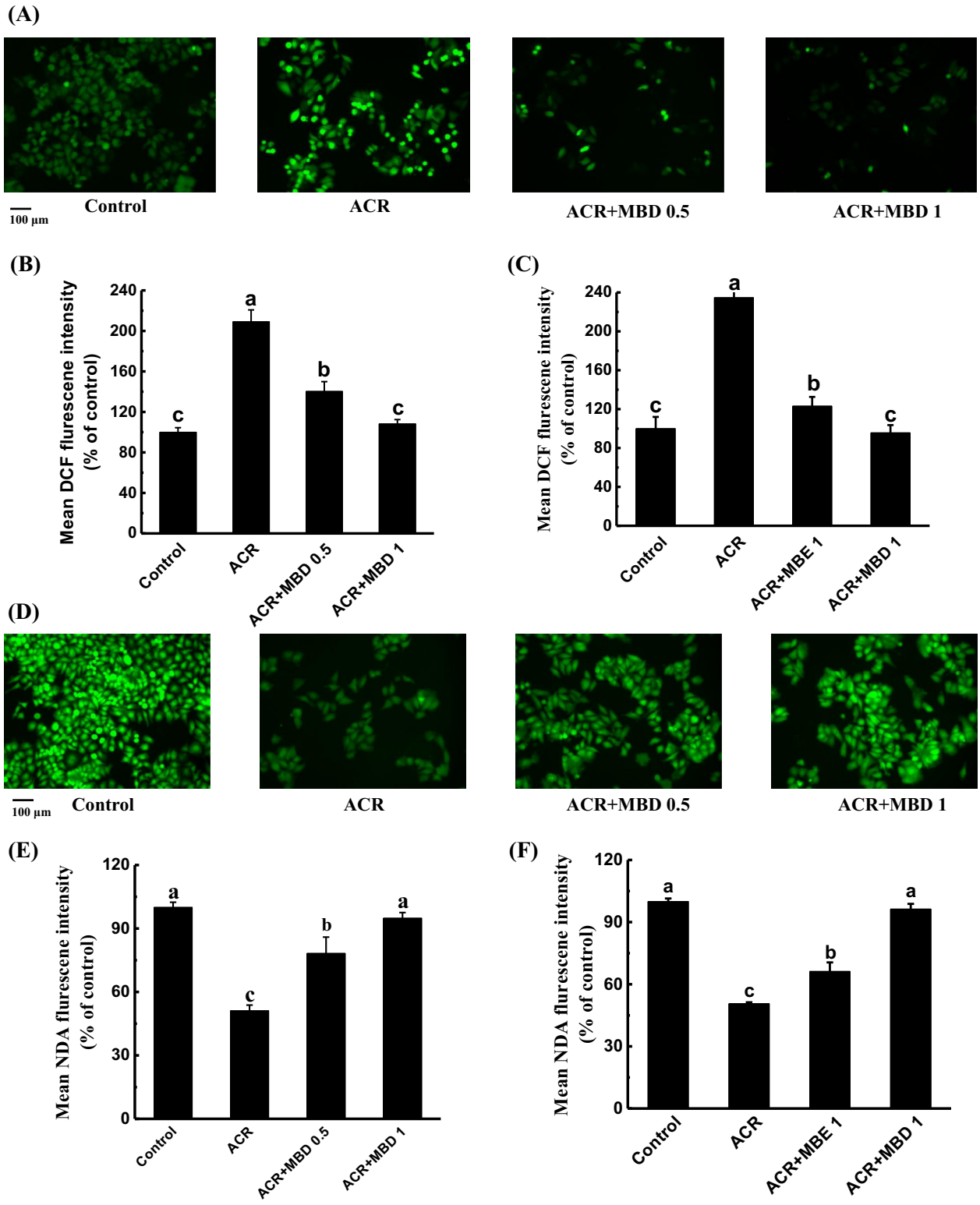

Fig. 2. Effect of MBD and MBE on ACR-induced ROS generation and GSH depletion in HepG2 cells. (A) Effect of MBD on ACR-induced ROS generation in HepG2 cells, after treatment with 5 mM ACR in the presence or absence of 0.5 mg/mL, 1 mg/mL of MBD for 24 h, cells were collected and incubated with 10 μM of DCFH-DA at 37 °C for 30 min, then cells were washed with PBS and measured by fluorescence microscope. (B) The quantitative data of panel (A) and the results were expressed as mean DCF fluorescence intensity ± standard deviations. (C) Effect of MBD and MBE on ACR-induced ROS generation in HepG2 cells, after treatment with 5 mM ACR in the presence or absence of 1 mg/mL of MBD or 1 mg/mL of MBE for 24 h, cells were collected and incubated with 10 μM of DCFH-DA at 37 °C for 30 min, then cells were washed with PBS and measured by fluorescence microscope. (D) Effect of MBD on ACR-induced depletion of GSH in HepG2 cells, after treatment with 5 mM of ACR in the presence or absence of 0.5 mg/mL, 1 mg/mL of MBD for 24 h, cells were collected and incubated with 10 μM of NDA at 37 °C for 30 min and then measured by fluorescence microscope. (E) The quantitative data of panel (D) and the results were expressed as mean NDA fluorescence intensity ± standard deviations. (F) Effect of MBD and MBE on ACR-induced GSH depletion in HepG2 cells, after treatment with 5 mM ACR in the presence or absence of 1 mg/mL of MBD or 1 mg/mL of MBE for 24 h, cells were collected and incubated with 10 μM of NDA at 37 °C for 30 min and then measured by fluorescence microscope. Different letters represent significant difference ($p < 0.05$). MBD, mulberry digest; MBE, mulberry extract; ACR, acrylamide; GSH, glutathione; NDA, naphthalene-2, 3-dicarboxal-dehyde. DCFH-DA, 2′,7′-dichlorofluorescin diacetate.

compounds, especially dihydroxy B-ring-substituted compounds, such as quercetin glycosides and cyanidin glycosides. These B-ring-substituted phenolic compounds are able to provide electrons and neutralize reactive oxygen species (Agati, Azzarello, Pollastri, & Tattini, 2012; Harborne, 1986; Chen, Xu, Zhang, Su & Zheng, 2016). Therefore, the effect on inhibiting ACR-induced ROS overproduction may be partially attributed to the various phenolic compounds in MBD and MBE.

3.4. Effect of MBD on the level of intracellular glutathione (GSH)

Glutathione (GSH) was considered as a protective agent against oxidative stress (D'Autreaux and Toledano, 2007). The overproduction of ROS was related to the level of intracellular GSH. The decreased level of GSH could not completely scavenge excessive ROS. It is clear from our study that MBD successfully suppressed the overproduction of ROS, and we assumed that these results could be associated with increased level of intracellular GSH. To test this hypothesis, the GSH level was measured in the presence or absence of MBD using NDA fluorescence probe. As shown in Fig. 2D and E, the depletion of GSH was evident after incubation with ACR. The fluorescence intensity was plunged to 51.14% ± 2.67% compared with control group. However, when HepG2 cells were pretreated with MBD for 24 h, the status was reversed. The fluorescence intensities of 0.5 mg/mL and 1 mg/mL of MBD were recovered to 78.25% ± 7.69% and 94.87% ± 2.68%, respectively. Significant differences were observed among these groups, and evidenced that both 0.5 mg/mL and 1 mg/mL of MBD provided protection against GSH depletion induced by ACR, and 1 mg/mL of MBD conferred stronger protection than that of 0.5 mg/mL of MBD. Combining with the effect of MBD on ROS and on GSH level, we conclude that pretreatment of cells with MBD potentially restored the level of GSH, and enhanced the resistance against oxidative stress. However, as we can see from Fig. 2F and Supplementary Fig. 8C-8D, mulberry fruits without digestion (MBE, 1 mg/mL) showed slight protection against ACR-induced GSH depletion compared with that of MBD, their fluorescence intensities were 66.19% ± 4.37% (MBE) and 96.30% ± 2.52% (MBD). These results indicated that the protective effect of mulberry fruits on ACR-induced GSH depletion could be enhanced after *in vitro* digestion.

3.5. Effect of MBD on ACR-induced mitochondrial dysfunction

Mitochondrion where ROS is generated principally, plays an important role in cellular ROS homeostasis (Trushina & McMurray, 2007). Interestingly, the inner mitochondrial membrane also incorporates an extensive antioxidant defense system, such as glutathione, vitamin E and ascorbate, to avoid cell injury caused by the generation of ROS (Lin & Beal, 2006; Reddy, 2006). Consequently, the overproduction of ROS may be associated with mitochondrial dysfunction, such as mitochondrial membrane potential (MMP) decrease and mitochondrial membrane lipid peroxidation. In our experiment, the enhanced ROS level and decreased GSH level were detected after incubation with ACR. These phenomena may be related to mitochondrial dysfunction. Therefore, we investigated that whether exposure to ACR could cause MMP decrease *via* RH123 fluorescence probe. As shown in Fig. 3A and B, the fluorescence intensity was decreased to 67.24% ± 4.80% compared with control group, which demonstrated that MMP was declined after treatment with ACR. Subsequently we evaluated the protective effect of MBD against ACR-induced MMP decrease. In presence of 0.5 mg/mL and 1 mg/mL of MBD, the fluorescence intensities of these two groups were increased as compared ACR alone treated group. Their fluorescence intensities recovered to 76.93 ± 1.87% and 89.89 ± 1.79% respectively. 1 mg/mL of MBD treatment group was more effective in attenuating ACR-induced MMP decrease than 0.5 mg/mL of MBD treatment group. Similarly, the effect of MBE on ACR-induced MMP decrease was also investigated. As we can see from Fig. 3C and Supplementary Fig. 9A-9B, after treatment with MBE (1 mg/mL), the fluorescence intensity recovered to 82.75% ± 1.40%, but lower than that of MBD (90.75% ± 1.47%), suggesting that MBD was better than MBE in inhibiting ACR-induced MMP decrease. In addition, the status of mitochondrial membrane lipid peroxidation was determined because ROS overproduction may lead to membrane lipid peroxidation. Similar results were observed in Fig. 3D–3F and Supplementary Fig. 9C-9D, namely ACR facilitated the peroxidation of mitochondrial membrane lipid, while MBD ameliorated lipid peroxidation in a dose-dependent manner and the protective effect of MBD treatment (1 mg/mL) was better than that of MBE (1 mg/mL). Mitochondrial damage caused by MMP decrease or membrane lipid peroxidation is a prerequisite for ROS production. Once this occurs, a vicious cycle that excessive ROS can further damage mitochondria would take place, thus leading to more ROS generation and depletion of antioxidant defense system (Lin, et al., 2006). Therefore, our results suggest that both MBD and MBE could significantly inhibit the ROS associated mitochondrial dysfunction, and the protective effect of MBD is better.

3.6. Effect of MBD on the enzyme activities of CAT and SOD

It is well established that increasing or preserving antioxidant enzyme activities, such as SOD and CAT, can resist oxidative stress (Movahed, Yu, Thandapilly, Louis, & Netticadan, 2012). Therefore, we evaluated that whether protective effect of MBD was associated with enzyme activities. As shown in Fig. 4A and 4C, significant decrease of CAT activity and SOD activity were observed in ACR exposure groups in comparison to control groups. Pretreatment with MBD markedly prevented the reduction in CAT activities in a dose-dependent manner, while SOD activity was not significantly improved between ACR-treated group and MBD-treated groups. As for MBE pretreatment, it can been seen from Fig. 4B and 4D that MBE treatment cannot inhibit the reduction in CAT activities or in SOD activities. These results jointly indicated that MBE displayed no significant protective effect on CAT or SOD enzyme activities, while the protective effect of MBD against ACR-induced oxidative stress was primarily attributed to the increased CAT activity rather than SOD activity in terms of antioxidant enzyme activities.

3.7. Effect of MBD on the level of ACR

In this study, we have confirmed that maintaining mitochondrial function and increasing CAT activities are partially responsible for MBD-mediated alleviation of oxidative damage. However, some studies considered that some protective agents afforded protection through direct reaction with toxins. For example, resveratrol may protect cardiomyocytes from oxidative damage directly by decreasing H_2O_2 (Movahed et al., 2012). Due to the complexity of MBD components, we speculated that MBD may directly react with ACR, thereby reducing the ACR-induced toxicity. To verify this speculation, 5 mM of ACR was incubated with different concentrations of MBD (0.25 mg/mL, 0.5 mg/mL, 1 mg/mL) at 37 °C. After incubation for 12 h and 24 h, the concentration of ACR was detected by HPLC. The results were summarized in Table 2 and Supplementary Fig. 10. Incubation with MBD for 12 h or 24 h has no effect on the depletion of ACR. Besides, among different concentration of MBD groups, there were also no significant change observed in term of ACR concentration. These results jointly demonstrated that MBD could not directly react with ACR. Consequently, the protective effect of MBD against ACR-induced oxida-

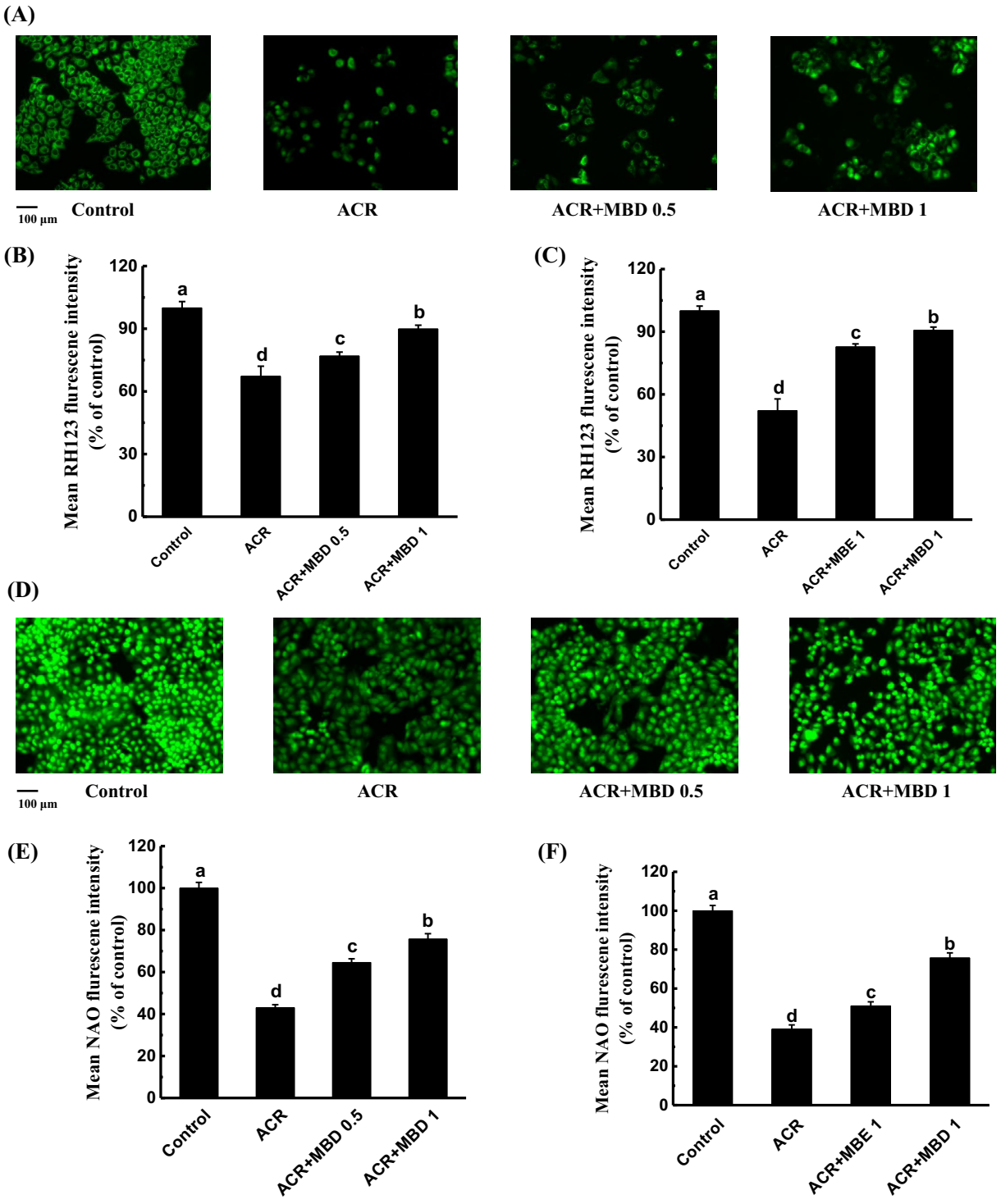

Fig. 3. Effect of MBD and MBE on ACR-induced mitochondrial membrane potential (MMP) decrease and mitochondrial membrane lipid peroxidation in HepG2 cells. (A) Effect of MBD on ACR-induced mitochondrial membrane potential (MMP) decrease in HepG2 cells, after treatment with 5 mM of ACR in the presence or absence of 0.5 mg/mL, 1 mg/mL of MBD for 24 h, cells were collected and incubated with 10 μM of RH123 at 37 °C for 30 min and then cells were washed with PBS and measured by fluorescence microscope. (B) The quantitative data of panel (A) and the results were expressed as mean RH123 fluorescence intensity ± standard deviations. (C) Effect of MBD and MBE on ACR-induced mitochondrial membrane potential (MMP) decrease in HepG2 cells, after treatment with 5 mM ACR in the presence or absence of 1 mg/mL of MBD or 1 mg/mL of MBE for 24 h, cells were collected and incubated with 10 μM of RH123 at 37 °C for 30 min and then cells were washed with PBS and measured by fluorescence microscope. (D) Effect of MBD on ACR-induced mitochondrial membrane lipid peroxidation in HepG2 cells, after treatment with 5 mM of ACR in the presence or absence of 0.5 mg/mL, 1 mg/mL of MBD for 24 h, cells were collected and incubated with 10 μM of NAO at 37 °C for 30 min and then measured by fluorescence microscope. (E) The quantitative data of panel (D) and the results were expressed as mean NAO fluorescence intensity ± standard deviations. (F) Effect of MBD and MBE on ACR-induced mitochondrial membrane lipid peroxidation in HepG2 cells, after treatment with 5 mM ACR in the presence or absence of 1 mg/mL of MBD or 1 mg/mL of MBE for 24 h, cells were collected and incubated with 10 μM of NAO at 37 °C for 30 min and then measured by fluorescence microscope. Different letters represent significant difference ($p < 0.05$). MBD, mulberry digest; MBE, mulberry extract; ACR, acrylamide; NAO, nonyl Acridine Orange; RH123, rhodamine 123.

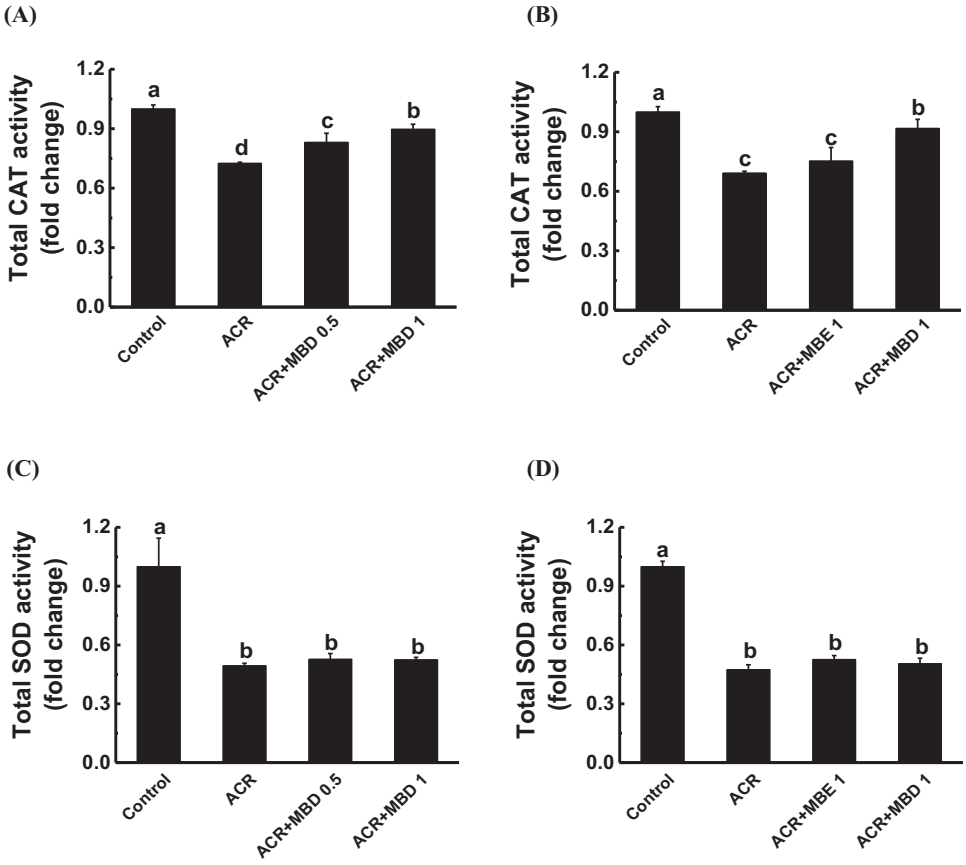

Fig. 4. Effect of MBD and MBE on CAT activity and SOD activity in HepG2 cells. (A) Effect of different concentrations (0.5 mg/mL and 1 mg/mL) of MBD on CAT activity, (B) Effect of MBD (1 mg/mL) and MBE (1 mg/mL) on CAT activity. (C) Effect of different concentrations (0.5 mg/mL and 1 mg/mL) of MBD on SOD activity, (D) Effect of MBD (1 mg/mL) and MBE (1 mg/mL) on SOD activity. The results were expressed as the fold of CAT activity or SOD activity of control group. Different letters represent significant difference ($p < 0.05$). MBD, mulberry digest; MBE, mulberry extract; CAT, catalase; SOD, superoxide dismutase.

Table 2
Effect of different concentrations of MBD on the concentration of ACR.

Group	Acrylamide concentration (mM)	
	12 h	24 h
Control (ACR, 5 mM)	4.94 ± 0.31	5.01 ± 0.33
ACR (5 mM) + MBD (0.25 mg/mL)	4.79 ± 0.29	4.91 ± 0.36
ACR (5 mM) + MBD (0.5 mg/mL)	4.87 ± 0.30	4.97 ± 0.34
ACR (5 mM) + MBD (1 mg/mL)	4.97 ± 0.21	5.04 ± 0.24

tive damage may be attributed to the increased cellular antioxidant capacity rather than the direct reaction with ACR.

4. Conclusion

The present study unveiled major phenolic compounds of mulberry digest (MBD) and their concentrations, namely quercetin rhamnosylhexoside hexoside (11.05 ± 1.10 mg/kg FW), quercetin-3-*O*-rutinoside (53.95 ± 2.21 mg/kg FW), quercetin hexoside (5.76 ± 0.45 mg/kg FW), kaempferol rhamnosylhexoside (4.93 ± 0.58 mg/kg FW), cyanidin-3-*O*-glucoside (497.28 ± 6.81 mg/kg FW) and cyanidin-3-*O*-rutinoside (287.20 ± 9.58 mg/kg FW). After digestion, the contents of four flavonoid glycosides were all increased, while the contents of two anthocyanins were both decreased significantly. The protective effects of MBD on ACR-induced cytotoxicity and genotoxicity were confirmed. MBD was capable of decreasing ROS generation, inhibiting MMP decrease, membrane lipid peroxidation, depletion of GSH, as well as increasing CAT activity. More interestingly, the protective effect of MBD against acrylamide-induced oxidative damage was enhanced compared with mulberry fruits without digestion (MBE). In addition, further study indicated that the protective mechanism of MBD may be primarily attributed to the enhanced ability to resist oxidative stress rather than the direct reaction with ACR. In conclusion, MBD can effectively attenuate ACR-induced oxidative damage, which might have implication for preventing health problems caused by dietary ACR exposure.

Conflict of interest

The authors declare that there are no conflicts of interest.

Acknowledgments

This work was supported by Grants from National Key Technology R&D Program of China (No.2016YFD0401201), the Fundamental Research Funds for the Central Universities (2017) and Research Foundation of the Education Department of Zhejiang Province (Y201328143).

Appendix A. Supplementary data

Supplementary data associated with this article can be found, in the online version, at http://dx.doi.org/10.1016/j.foodchem.2017.03.045.

References

Agati, G., Azzarello, E., Pollastri, S., & Tattini, M. (2012). Flavonoids as antioxidants in plants: Location and functional significance. *Plant Science, 196*, 67–76.

Cariddi, L. N., Sabini, M. C., Escobar, F. M., Bacchetti, R., Montironi, I., Merckis, C., et al. (2015). In vitro and in vivo cytogenotoxic effects of hot aqueous extract of *Achyrocline satureioides* (Lam.) DC. *BioMed Research International, 2015*. 270973-270973.

Chen, W., Feng, L., Nie, H., & Zheng, X. (2012). Andrographolide induces autophagic cell death in human liver cancer cells through cyclophilin D-mediated mitochondrial permeability transition pore. *Carcinogenesis, 33*(11), 2190–2198.

Chen, W., Feng, L., Shen, Y., Su, H., Li, Y., Zhuang, J., et al. (2013a). Myricitrin inhibits acrylamide-mediated cytotoxicity in human Caco-2 cells by preventing oxidative stress. *BioMed Research International, 2013*. 724183.

Chen, W., Li, Y., Li, J., Han, Q., Ye, L., & Li, A. (2011). Myricetin affords protection against peroxynitrite-mediated DNA damage and hydroxyl radical formation. *Food and Chemical Toxicology, 49*(9), 2439–2444.

Chen, W., Shen, Y., Su, H., & Zheng, X. (2014). Hispidin derived from *Phellinus linteus* affords protection against acrylamide-induced oxidative stress in Caco-2 cells. *Chemico-Biological Interactions, 219*, 83–89.

Chen, W., Su, H., Huang, Z., Feng, L., & Nie, H. (2012). Neuroprotective effect of raspberry extract by inhibiting peroxynitrite-induced DNA damage and hydroxyl radical formation. *Food Research International, 49*(1), 22–26.

Chen, W., Su, H., Xu, Y., Bao, T., & Zheng, X. (2016). Protective effect of wild raspberry (*Rubus hirsutus Thunb.*) extract against acrylamide-induced oxidative damage is potentiated after simulated gastrointestinal digestion. *Food Chemistry, 196*, 943–952.

Chen, W., Xu, Y., Zhang, L., Su, H., & Zheng, X. (2016). Blackberry subjected to in vitro gastrointestinal digestion affords protection against Ethyl Carbamate-induced cytotoxicity. *Food Chemistry, 212*, 620–627.

Chen, W., Zhao, Z., & Li, Y. (2011). Simultaneous increase of mycelial biomass and intracellular polysaccharide from Fomes fomentarius and its biological function of gastric cancer intervention. *Carbohydrate Polymers, 85*(2), 369–375.

Chen, W., Zhao, Z., Li, L., Wu, B., Chen, S.-F., Zhou, H., et al. (2008). Hispolon induces apoptosis in human gastric cancer cells through a ROS-mediated mitochondrial pathway. *Free Radical Biology and Medicine, 45*(1), 60–72.

Chen, W., Zhuang, J., Li, Y., Shen, Y., & Zheng, X. (2013b). Myricitrin protects against peroxynitrite-mediated DNA damage and cytotoxicity in astrocytes. *Food Chemistry, 141*(2), 927–933.

D'Autreaux, B., & Toledano, M. B. (2007). ROS as signalling molecules: Mechanisms that generate specificity in ROS homeostasis. *Nature Reviews Molecular Cell Biology, 8*(10), 813–824.

De Rosso, M., Panighel, A., Vedova, A. D., Gardiman, M., & Flamini, R. (2015). Characterization of non-anthocyanic flavonoids in some hybrid red grape extracts potentially interesting for industrial uses. *Molecules, 20*(10), 18095–18106.

Halliwell, B. (2006). Oxidative stress and neurodegeneration: Where are we now? *Journal of Neurochemistry, 97*(6), 1634–1658.

Harborne, J. B. (1986). Nature, distribution and function of plant flavonoids. *Progress in Clinical and Biological Research, 213*, 15–24.

Kang, M.-C., Kin, K.-N., Wijesinghe, W. A. J. P., Yang, X., Ahn, G., & Jeon, Y. J. (2014). Protective effect of polyphenol extracted from Ecklonia cava against ethanol induced oxidative damage in vitro and in zebrafish model. *Journal of Functional Foods, 6*, 339–347.

Kremer Faller, A. L., Fialho, E., & Liu, R. H. (2012). Cellular antioxidant activity of Feijoada whole meal coupled with an in vitro digestion. *Journal of Agricultural and Food Chemitry, 60*(19), 4826–4832.

Lin, M. T., & Beal, M. F. (2006). Mitochondrial dysfunction and oxidative stress in neurodegenerative diseases. *Nature, 443*(7113), 787–795.

Liu, L.-K., Chou, F.-P., Chen, Y.-C., Chyau, C.-C., Ho, H.-H., & Wang, C.-J. (2009). Effects of mulberry (*Morus alba* L.) extracts on lipid homeostasis in vitro and in vivo. *Journal of Agricultural and Food Chemitry, 57*(16), 7605–7611.

McDougall, G. J., Fyffe, S., Dobson, P., & Stewart, D. (2007). Anthocyanins from red cabbage – stability to simulated gastrointestinal digestion. *Phytochemistry, 68*(9), 1285–1294.

Mehri, S., Abnous, K., Mousavi, S. H., Shariaty, V. M., & Hosseinzadeh, H. (2012). Neuroprotective effect of crocin on acrylamide-induced cytotoxicity in PC12 cells. *Cellular and Molecular Neurobiology, 32*(2), 227–235.

Movahed, A., Yu, L., Thandapilly, S. J., Louis, X. L., & Netticadan, T. (2012). Resveratrol protects adult cardiomyocytes against oxidative stress mediated cell injury. *Archives of Biochemistry and Biophysics, 527*(2), 74–80.

Natic, M. M., Dabic, D. C., Papetti, A., Fotiric Aksic, M. M., Ognjanov, V., Ljubojevic, M., et al. (2015). Analysis and characterisation of phytochemicals in mulberry (Morus alba L.) fruits grown in Vojvodina. *North Serbia. Food Chemistry, 171*, 128–136.

Ortega, N., Reguant, J., Romero, M.-P., Macia, A., & Motilva, M.-J. (2009). Effect of fat content on the digestibility and bioaccessibility of cocoa polyphenol by an in vitro digestion model. *Journal of Agricultural and Food Chemitry, 57*(13), 5743–5749.

Orwar, O., Fishman, H. A., Ziv, N. E., Scheller, R. H., & Zare, R. N. (1995). Use of 2,3-naphthalenedicarboxaldehyde derivatization for single-cell analysis of glutathione by capillary electrophoresis and histochemical-localization ion by fluorescence microscopy. *Analytical Chemistry, 67*(23), 4261–4268.

Prasad, S. N., & Muralidhara (2012). Evidence of acrylamide induced oxidative stress and neurotoxicity in Drosophila melanogaster – Its amelioration with spice active enrichment: Relevance to neuropathy. *Neurotoxicology, 33*(5), 1254–1264.

Reddy, P. H. (2006). Amyloid precursor protein-mediated free radicals and oxidative damage: Implications for the development and progression of Alzheimer's disease. *Journal of Neurochemistry, 96*(1), 1–13.

Rodriguez-Ramiro, I., Ramos, S., Bravo, L., Goya, L., & Angeles Martin, M. (2011). Procyanidin B2 and a cocoa polyphenolic extract inhibit acrylamide-induced apoptosis in human Caco-2 cells by preventing oxidative stress and activation of JNK pathway. *Journal of Nutritional Biochemistry, 22*(12), 1186–1194.

Saura-Calixto, F., & Diaz-Rubio, M. E. (2007). Polyphenols associated with dietary fibre in wine – A wine polyphenols gap? *Food Research International, 40*(5), 613–619.

Shan, X., Li, Y., Meng, X., Wang, P., Jiang, P., & Feng, Q. (2014). Curcumin and (-)-epigallocatechin-3-gallate attenuate acrylamide-induced proliferation in HepG2 cells. *Food and Chemical Toxicology, 66*, 194–202.

Trachootham, D., Zhou, Y., Zhang, H., Demizu, Y., Chen, Z., Pelicano, H., et al. (2006). Selective killing of oncogenically transformed cells through a ROS-mediated mechanism by beta-phenylethyl isothiocyanate. *Cancer Cell, 10*(3), 241–252.

Trushina, E., & McMurray, C. T. (2007). Oxidative stress and mitochondrial dysfunction in neurodegenerative diseases. *Neuroscience, 145*(4), 1233–1248.

Wang, H., Lee, A. W. M., Shuang, S., & Choi, M. M. F. (2008). SPE/HPLC/UV studies on acrylamide in deep-fried flour-based indigenous Chinese foods. *Microchemical Journal, 89*(2), 90–97.

Wojdylo, A., Nowicka, P., Laskowski, P., & Oszmianski, J. (2014). Evaluation of sour cherry (*Prunus cerasus* L.) fruits for their polyphenol content, antioxidant properties, and nutritional components. *Journal of Agricultural and Food Chemitry, 62*(51), 12332–12345.

Wu, T., Qi, X., Liu, Y., Guo, J., Zhu, R., Chen, W., et al. (2013a). Dietary supplementation with purified mulberry (*Morus australis* Poir) anthocyanins suppresses body weight gain in high-fat diet fed C57BL/6 mice. *Food Chemistry, 141*(1), 482–487.

Wu, T., Tang, Q., Gao, Z., Yu, Z., Song, H., Zheng, X., et al. (2013b). Blueberry and mulberry juice prevent obesity development in C57BL/6 Mice. *PLoS ONE, 8*(10).

Yan, F., Zhang, J., Zhang, L., & Zheng, X. (2016). Mulberry anthocyanin extract regulates glucose metabolism by promotion of glycogen synthesis and reduction of gluconeogenesis in human HepG2 cells. *Food & Function, 7*(1), 425–433.

Yang, X., Yang, L., & Zheng, H. (2010). Hypolipidemic and antioxidant effects of mulberry (Morus alba L.) fruit in hyperlipidaemia rats. *Food and Chemical Toxicology, 48*(8–9), 2374–2379.

Zhang, L., Zhang, H., Miao, Y., Wu, S., Ye, H., & Yuan, Y. (2012). Protective effect of allicin against acrylamide-induced hepatocyte damage in vitro and in vivo. *Food and Chemical Toxicology, 50*(9), 3306–3312.